Numerical computation of dispersion relations for multi-layered anisotropic structures

N. D. Botkin, K.-H. Hoffmann, O. A. Pykhteev and V. L. Turova

Ludwig-Erhard-Allee 2, 53175 Bonn, Germany, e-mail: pykhteev@caesar.de

ABSTRACT

The paper presents an algorithm and a program for the computation of the velocity of acoustic waves excited in anisotropic multi-layered structures. The investigation is motivated by modeling of a biosensor which serves for the detection and quantitative measurement of microscopic amounts of biological substances. The program is supplied with a user friendly graphical interface and can be useful for researchers working on acoustic sensors.

Keywords: dispersion relations, surface acoustic waves, multi-layered structures, linear elasticity.

1 INTRODUCTION

The paper outlines an algorithm and a program for the computation of the velocity of acoustic waves excited in anisotropic multi-layered structures. In contrast to acoustic waves in bulk materials, the wave velocity in laminate structures depends on the frequency because of the interaction between the layers with different acoustic properties. Therefore, one can speak about dispersion relations that express the connection between the velocity and the frequency of acoustic waves.

The investigation of dispersion relations is motivated by the modeling of a biosensor [1] that serves for the detection and quantitative measurement of microscopic amounts of biological substances. The operating principle of the biosensor is based on the generation and detection of horizontally polarized shear Love waves. From the mechanical point of view, the biosensor is a multi-layered structure consisting both of isotropic and anisotropic layers. The biological substance adheres to the surface of the top layer so that a new layer is being formed, which changes the velocity of shear waves propagating along the sensor's surface. Thus, an effective tool for computing the velocity of waves in multi-layered structures would enable us to estimate the sensitivity of the biosensor in dependence on its constructive features and operation parameters.

Classical examples of the derivation of dispersion relations demonstrate that the problem is solvable analytically in simplest cases only (see e.g. [2]). Therefore, it is reasonable to examine semi-analytical methods that use both analytical representations of solutions and numerical determination of their parameters. Such a method and the related program are developed by the authors. The algorithm is based on the construction of travelling wave solutions of elasticity equations describing deformations in the layers. The wave velocity is computed from the fitting of mechanical conditions on the interfaces between the layers. These conditions express the continuity of the displacement field and the pressure equilibrium for each pair of the layers. Feasible wave velocities are the roots of a non-negative real function (fitting function) that expresses a measure of the inconsistence in the interface conditions. Comparing with other existing developments (e.g. [3]) our program is especially effective in the case of very thin layers.

2 MATHEMATICAL MODEL

2.1 Simple structure

First, consider a simplified structure shown in Figure 1. Here, an anisotropic layer lies on an anisotropic half-space substrate. The fluid is not present in the model. The computation of the velocity of surface acoustic waves is based on the construction of travelling wave solutions that exponentially decrease with x_3.

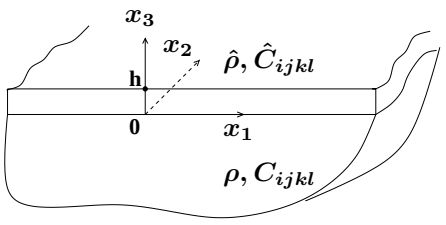

Figure 1: A sample structure. Here, $\hat{\rho}$, ρ, and $\hat{C}_{ijkl}$, C_{ijkl} are the densities and the elastic stiffness tensors, respectively.

The elasticity equations for the substrate and the top layer read:

$$\rho u_{i\,tt} - C_{ijkl}\frac{\partial^2 u_l}{\partial x_j \partial x_k} = 0,\ i = 1,2,3, \tag{1}$$

$$\hat{\rho}\hat{u}_{i\,tt} - \hat{C}_{ijkl}\frac{\partial^2 \hat{u}_l}{\partial x_j \partial x_k} = 0,\ i = 1,2,3, \tag{2}$$

where u_i and $\hat{u}_i$, $i = 1, 2, 3$, are components of the displacement vectors. A plain wave propagating in the structure in x_1 direction is of the form:

$$u_i(x_1, x_3) = a_i(x_3)\cos(\kappa x_1 - \omega t) + b_i(x_3)\sin(\kappa x_1 - \omega t), \quad (3)$$

$$\hat{u}_i(x_1, x_3) = \hat{a}_i(x_3)\cos(\kappa x_1 - \omega t) + \hat{b}_i(x_3)\sin(\kappa x_1 - \omega t). \quad (4)$$

Here, κ is the wave number, ω the circuit frequency. The substitution of (3) and (4) into (1) and (2), respectively, yields

$$-C_{i33l}\,\ddot{a}_l - (C_{i13l} + C_{i31l})\,\dot{b}_l + C_{i11l}\,a_l - \rho\frac{\omega^2}{\kappa^2}\,a_i = 0,$$

$$-C_{i33l}\,\ddot{b}_l + (C_{i13l} + C_{i31l})\,\dot{a}_l + C_{i11l}\,b_l - \rho\frac{\omega^2}{\kappa^2}\,b_i = 0,$$

$$-\hat{C}_{i33l}\,\ddot{\hat{a}}_l - (\hat{C}_{i13l} + \hat{C}_{i31l})\,\dot{\hat{b}}_l + \hat{C}_{i11l}\,\hat{a}_l - \hat{\rho}\frac{\omega^2}{\kappa^2}\,\hat{a}_i = 0,$$

$$-\hat{C}_{i33l}\,\ddot{\hat{b}}_l + (\hat{C}_{i13l} + \hat{C}_{i31l})\,\dot{\hat{a}}_l + \hat{C}_{i11l}\,\hat{b}_l - \hat{\rho}\frac{\omega^2}{\kappa^2}\,\hat{b}_i = 0.$$

Here, $i = 1, 2, 3$, the dot denotes the differentiation with respect to the variable $\tilde{x}_3 = \kappa x_3$. With the state vectors

$$\vec{q} = (a_1, a_2, a_3, b_1, b_2, b_3, \dot{a}_1, \dot{a}_2, \dot{a}_3, \dot{b}_1, \dot{b}_2, \dot{b}_3)^T \in R^{12},$$

$$\hat{\vec{q}} = (\hat{a}_1, \hat{a}_2, \hat{a}_3, \hat{b}_1, \hat{b}_2, \hat{b}_3, \dot{\hat{a}}_1, \dot{\hat{a}}_2, \dot{\hat{a}}_3, \dot{\hat{b}}_1, \dot{\hat{b}}_2, \dot{\hat{b}}_3)^T \in R^{12},$$

the above systems can be rewritten in the normal form as follows:

$$\dot{\vec{q}} = A\,\vec{q}, \quad \dot{\hat{\vec{q}}} = \hat{A}\,\hat{\vec{q}}, \quad (5)$$

where A and $\hat{A}$ are the corresponding matrices. Let $\lambda_1, ..., \lambda_{12}$ and $\vec{h}_1, ..., \vec{h}_{12}$ (respectively, $\hat{\lambda}_1, ..., \hat{\lambda}_{12}$ and $\hat{\vec{h}}_1, ..., \hat{\vec{h}}_{12}$) be eigenvalues and eigenvectors of A (respectively, $\hat{A}$). One can verify that just ℓ linear independent eigenvectors can be found for each ℓ-multiple eigenvalue. Therefore, solutions of (5) are of the form: $\vec{q}(x_3) = \sum_{i=1}^{12} D_i \vec{h}_i e^{\lambda_i \kappa x_3}$, $\hat{\vec{q}}(x_3) = \sum_{i=1}^{12} \hat{D}_i \hat{\vec{h}}_i e^{\hat{\lambda}_i \kappa x_3}$, where D_i and $\hat{D}_i$ are arbitrary constants. Selecting solutions decreasing in the substrate yields:

$$\vec{q}(x_3) = \sum_{j=1}^{N} D_j \vec{h}_{i_j} e^{\lambda_{i_j} \kappa x_3}, \quad \text{Re}\ \lambda_{i_j} > 0.$$

Note that $N \le 6$ due to the up-down symmetry of the substrate. Solutions in the upper layer are assumed to be of the oscillatory type:

$$\hat{\vec{q}}(x_3) = \sum_{j=1}^{L} \hat{D}_j \hat{\vec{h}}_{i_j} e^{\hat{\lambda}_{i_j} \kappa x_3}, \quad \text{Re}\ \hat{\lambda}_{i_j} = 0.$$

Thus,

$$a_l = \sum_{j=1}^{N} D_j h_{i_j}^{(l)} e^{\lambda_{i_j} \kappa x_3}, \quad b_l = \sum_{j=1}^{N} D_j h_{i_j}^{(l+3)} e^{\lambda_{i_j} \kappa x_3},$$

$$\hat{a}_l = \sum_{j=1}^{L} \hat{D}_j \hat{h}_{i_j}^{(l)} e^{\hat{\lambda}_{i_j} \kappa x_3}, \quad \hat{b}_l = \sum_{j=1}^{L} \hat{D}_j \hat{h}_{i_j}^{(l+3)} e^{\hat{\lambda}_{i_j} \kappa x_3},$$

where l runs from 1 to 3. Therefore, the displacements u_i and $\hat{u}_i$, see (3) and (4), depend linearly on $D_r, r = 1, N$, and $\hat{D}_s$, $s = 1, L$, respectively.

For all x_1 and t, the following interface conditions must hold:

$$u_i = \hat{u}_i, \quad \text{at } x_3 = 0, \ \text{continuity}; \quad (6)$$

$$C_{i3kl}\frac{\partial u_l}{\partial x_k} = \hat{C}_{i3kl}\frac{\partial \hat{u}_l}{\partial x_k}, \ \text{at } x_3 = 0, \ \text{equilibrium of pressures}; \quad (7)$$

$$\hat{C}_{i3kl}\frac{\partial \hat{u}_l}{\partial x_k} = 0, \quad \text{at } x_3 = h, \ \text{free of forces boundary}. \quad (8)$$

The above system yields 18 linear equations for $N + L \le 18$ coefficients D_r and $\hat{D}_s$. Note that $N + L < 18$ as a rule. Let $V = \omega/\kappa$ be the unknown wave velocity and $G(V)$ the $18 \times (N + L)$-matrix of the above system. Feasible wave velocities are determined from the condition of nontrivial solvability for the system $G(V)\vec{D} = 0$, where $\vec{D} = (D_1, ...D_N, \hat{D}_1, ...\hat{D}_L)^T$. Thus, the condition $rank\, G(V) < N + L$ holds for the feasible velocities, which is equivalent to the following condition: $\det\left|\bar{G}^T(V)G(V)\right| = 0$. The last equation can be easily solved because the computation of the left-hand-side runs very quickly even on an ordinary computer. Usually, three roots are being found whenever the layers are sufficiently thin, which corresponds to three wave types that propagate with different velocities. The selection of the desired wave type is quite obvious because the relation between their velocities is usually known.

2.2 Introducing a fluid

Assume now that the surface of the top layer of the structure shown in Figure 1 contacts with a viscose, weakly compressible fluid. The Stokes equations for compressible viscous fluids read:

$$\varrho v_{i\,t} - \nu\Delta v_i - (\zeta + \frac{\nu}{3})\frac{\partial}{\partial x_i}\mathrm{div}\,\vec{v} + \frac{\partial}{\partial x_i}p = 0,$$

$$\varrho_t + \frac{\partial}{\partial x_i}(\varrho v_i) = 0,$$

where ϱ is the density of the fluid, $v_i, i = 1, 2, 3$, are components of the velocity field, p is the static pressure, ν and ζ are the dynamic and volume viscosities of the fluid, respectively. The weak compressibility means that

$$\varrho(p) \approx \varrho_0 + \alpha \cdot p, \quad \varrho_0 = \varrho(0), \quad \alpha = \frac{\partial \varrho}{\partial p}(0),$$

which yields the following linearized equations:

$$\varrho_0 v_{i\,t} - \nu\Delta v_i - (\zeta + \frac{\nu}{3})\frac{\partial}{\partial x_i}\mathrm{div}\,\vec{v} + \frac{\partial}{\partial x_i}p = 0, \quad (9)$$

$$\alpha p_t + \varrho_0 \frac{\partial}{\partial x_i} v_i = 0. \tag{10}$$

Similar to the case of section 2.1, consider plain waves propagating in the fluid in x_1 direction:

$$v_i(x_1, x_3) = c_i(x_3)\cos(\kappa x_1 - \omega t) + d_i(x_3)\sin(\kappa x_1 - \omega t),$$
$$p(x_1, x_3) = e(x_3)\cos(\kappa x_1 - \omega t) + f(x_3)\sin(\kappa x_1 - \omega t).$$

Substituting this ansatz in (9) and (10) results in a system of linear ordinary differential equations for the determination of the amplitudes $c_i(x_3), d_i(x_3), i = 1, 2, 3$, $e(x_3)$, and $f(x_3)$. The amplitudes are being represented as linear combinations of exponents with arbitrary coefficients. The matching conditions at the interface between the fluid and the elastic layer consist in the continuity of the velocities and the equilibrium of the normal pressures:

$$v_i = \frac{\partial}{\partial t}\hat{u}_i, \tag{11}$$

$$\hat{C}_{i3kl}\frac{\partial \hat{u}_l}{\partial x_k} = -p\delta_{i3} + \nu\left(\frac{\partial v_i}{\partial x_3} + \frac{\partial v_3}{\partial x_i}\right) + (\zeta - \frac{2}{3}\nu)\delta_{i3}\,\mathrm{div}\,\vec{v}. \tag{12}$$

These relations replace equation (8) of the system (6)–(8). The system (6), (7), (8), (11), (12) is being treated as that is described in section 2.1.

2.3 Introducing piezoelectricity

Acoustic waves are usually excited through piezoelectric materials like α-quartz. Such materials can transform electric fields into deformations and vice versa so that deformations have influence on themselves through the electric field. Therefore, the propagation of waves depends on piezoelectric and electric properties of the layers. To explain how the piezoelectric effects can be taken into account, consider the following simple structure: I. Piezoelectric layer, II. Dielectric layer, III. Metallic layer. Because of small deformations, linear constitutive relations for piezoelectric materials are used:

$$\sigma_{ij} = C_{ijkl}\varepsilon_{kl} - e_{kij}E_k, \qquad D_i = \epsilon_{ij}E_j + e_{ikl}\varepsilon_{kl}.$$

Here, σ_{ij} and ε_{kl} are the stress and strain tensors, respectively; D_i and E_i denote the electric displacement and field, respectively; ε_{kl}, e_{kij}, and C_{ijkl} denote the material dielectric tensor, the stress piezoelectric tensor, and the elastic stiffness tensor, respectively.

Let ϕ be the potential function such that $E_i = \partial\phi/\partial x_i$, then the governing equations derived from the above constitutive relations read:

$$\rho^I u^I_{i\,tt} - C^I_{ijkl}\frac{\partial^2 u^I_l}{\partial x_j \partial x_k} + e^I_{kij}\frac{\partial^2 \phi^I}{\partial x_k \partial x_j} = 0,$$

$$\epsilon^I_{ij}\frac{\partial^2 \phi^I}{\partial x_i \partial x_j} + e^I_{ikl}\frac{\partial^2 u^I_l}{\partial x_i \partial x_k} = 0.$$

For dielectrics without piezoelectric properties, the stress piezoelectric tensor vanishes so that the elasticity equations and the equation determining the potential function are decoupled:

$$\rho^{II} u^{II}_{i\,tt} - C^{II}_{ijkl}\frac{\partial^2 u^{II}_l}{\partial x_j \partial x_k} = 0, \qquad \epsilon^{II}_{ij}\frac{\partial^2 \phi^{II}}{\partial x_i \partial x_j} = 0.$$

Metals are purely elastic so that we have

$$\rho^{III} u^{III}_{i\,tt} - C^{III}_{ijkl}\frac{\partial^2 u^{III}_l}{\partial x_j \partial x_k} = 0.$$

The conditions on the interface between the piezoelectric, dielectric, and metallic layers are the following:

$$C^I_{i3kl}\frac{\partial u^I_l}{\partial x_k} - e^I_{ki3}\frac{\partial \phi^I}{\partial x_k} = C^{II}_{i3kl}\frac{\partial u^{II}_l}{\partial x_k}, \qquad \text{interface I/II}$$

$$\epsilon^I_{3j}\frac{\partial \phi^I}{\partial x_j} + e^I_{3kl}\frac{\partial u^I_l}{\partial x_k} = \epsilon^{II}_{3j}\frac{\partial \phi^{II}}{\partial x_j}, \qquad \text{interface I/II}$$

$$C^{II}_{i3kl}\frac{\partial u^{II}_l}{\partial x_k} = C^{III}_{i3kl}\frac{\partial u^{III}_l}{\partial x_k}, \quad \phi^{II} = 0, \qquad \text{interface II/III.}$$

The technique described in subsection 2.1 can be applied to treat this case.

3 PROGRAM DESCRIPTION

The program is supplied with a user friendly graphical interface written in Visual C++. Using this interface, one can compose a multi-layered structure consisting of arbitrary number of isotropic and anisotropic layers. The material properties such as elastic stiffness tensors can easily be set and edited. If a layer is anisotropic, the orientation of its material is described in terms of successive rotations of the reference system. It is possible to import material parameters from existing models, which is especially convenient when dealing with elastic stiffness tensors containing a lot of coefficients. After composing the structure and specifying the wave frequency, the fitting function is computed and graphically presented (see Fig. 2). Now, the roots of the fitting function can be localized and found precisely along with polarization vectors that indicate the wave types. Moreover, the program possesses an option for the automatic computation of dispersion curves (dependences between the wave velocity and the frequency) for given frequency intervals. Such features make the program useful for researchers working on acoustic sensors.

4 EXAMPLES

Figure 3 shows a dispersion curve generated by the program for a simple structure consisting of a half-space isotropic substrate covered with an isotropic layer. For such a simple structure analytical solution can be found (see [2]). The squares mark points found analytically.

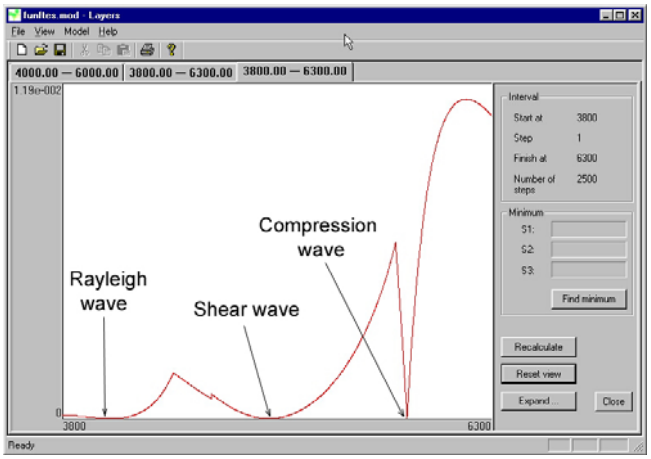

Figure 2: The main window of the program. Roots of the fitting function are the wave velocities for different wave types.

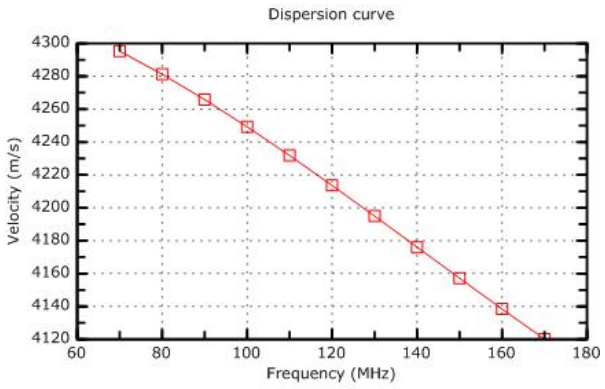

Figure 3: Dispersion curve generated by the program and points found analytically.

Figure 4 demonstrates the application of our method to the verification of physical experiments related to a biosensor developed at caesar [4]. A 9 nm copper film is deposited on the top layer of the biosensor. Curve (a) shows the time performance of the etching of the cooper film. The water flux is being alternated with the flux of an acid solution. The phase shift is being measured. Curve (b) represents the phase shift computed using dispersion relations. The simulation proves the assumption that the jump at the acid-to-water transition is caused by the change of the fluid viscosity.

5 CONCLUSION AND PERSPECTIVE

The methods presented in this paper are already successfully applied to the development of a biosensor at the research center caesar. Now, the investigation concerns the influence of bio-molecules deposited on the work surface of the biosensor on the waves propagation. Thus, a bristle structure consisting of the bio-molecules and moving in the fluid should be modeled. This can be

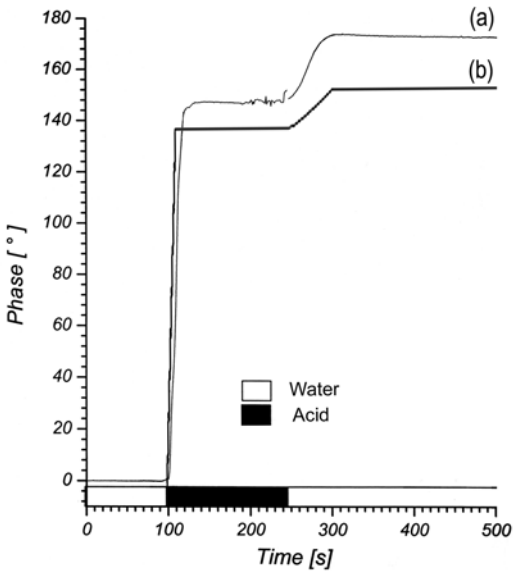

Figure 4: Verification of physical experiments through numerical simulations: (a) experiment, (b) simulation.

done through the homogenization technique described in [5]. The bristle structure is replaced with an averaged material whose properties are derived as the number of bristles goes to infinity whereas their thickness goes to zero. The computation of parameters of the averaged material will be included into the program.

Sometimes, investigated structures contain very much of periodically alternating layers whose thickness is significantly less than the wave length. Such a sandwich can be replaced by an averaged layer whose properties can be derived by means of the homogenization technique. Note that the homogenization will be performed in the transversal direction only. Therefore, explicit formulas for parameters of the averaged material can be obtain. This option will also be implemented.

REFERENCES

[1] N. Botkin, M. Schlensog, M. Tewes and V. Turova, "A mathematical model of a biosensor", Proc. MSM 2001, Hilton Head Island, 231–234, 2001.

[2] L.D. Landau and E.M. Lifschitz, "Elastizitätstheorie", Akademie–Verlag, Berlin, 1975.

[3] Pavlakovic, Lowe, Alleyne and Cawley, "Disperse: a general purpose program for creating dispersion curves", Annual review of progress in quantitative NDE (ed. Thompson and Chimenti), Plenum Press, New York, 155–192, 1997.

[4] Annual Report 2002, Center of Advanced European Studies and Research, Bonn (www.caesar.de).

[5] N.D. Botkin, K.-H. Hoffmann, V.N. Starovoitov and V.L. Turova, "Modeling the interaction between bristle elastic structures and fluids", Proc. MSM 2003, San Francisco, 126–129, 2003.